RSC Advances

This is an *Accepted Manuscript*, which has been through the Royal Society of Chemistry peer review process and has been accepted for publication.

Accepted Manuscripts are published online shortly after acceptance, before technical editing, formatting and proof reading. Using this free service, authors can make their results available to the community, in citable form, before we publish the edited article. This *Accepted Manuscript* will be replaced by the edited, formatted and paginated article as soon as this is available.

You can find more information about *Accepted Manuscripts* in the **Information for Authors**.

Please note that technical editing may introduce minor changes to the text and/or graphics, which may alter content. The journal's standard **Terms & Conditions** and the **Ethical guidelines** still apply. In no event shall the Royal Society of Chemistry be held responsible for any errors or omissions in this *Accepted Manuscript* or any consequences arising from the use of any information it contains.

Microwave synthesis of high rate nanostructured LiMnBO$_3$ with excellent cyclic behavior for lithium ion batteries

Kaliyappan Karthikeyan[a,b,*], Yun Sung. Lee[b,*]

RSC advances
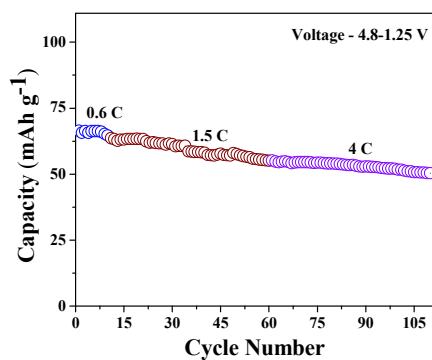
COMMUNICATION

Microwave synthesis of high rate nanostructured LiMnBO₃ with excellent cyclic behavior for lithium ion batteries

Kaliyappan Karthikeyan[a,b,*], Yun Sung. Lee[b,*]

The LiMnBO₃ nanobeads (LMB-NB) prepared using urea assisted microwave irradiation method delivered 67 mAh g⁻¹ capacity at 0.6 C rate between 1.25 and 4.8 V, showing 88 % of cyclability after 100 cycles. In addition, LMB-NB electrode also showed superior rate capability with 63 and 55 mAh g⁻¹ capacity at 1.5 and 4 C rates, which is the best ever reported rate performance for LiMnBO₃ material.

Recently, many effects have been made to replace layered $LiCoO_2$ cathode material for large scale lithium ion batteries (LIB) application. In spite of considering other layered $LiMO_2$ (M=Ni and Mn), $Li(Mn_{1/3}Ni_{1/3}Co_{1/3})O_2$ olivine type, Li_2MnO3, $LiMn_2O_4$ and $LiNi_{0.5}Mn_{1.5}O_2$ as possible alternatives, these materials have their own shortcomings, which prevent them to be applied in LIB for electric and hybrid electric vehicles. [1-3] Consequently, it is also very important to develop energy sources materials with desirable features like less toxicity, low cost, large theoretical capacity, high chemical and thermal stability. Moreover, the progress of exploring new energy source materials along with high electrochemical performance is also a major challenge for the advancement of LIB in future. [4]

In this line of research, lithium metal borates ($LiMBO_3$, M=Mn or Fe) is attracting more researchers due to the stable polyanion group, high thermal stability, comparable density, electrochemical stability because of small volume changes and its higher theoretical capacity (< 220 mA h⁻¹) than other electrode materials like $LiMO_2$ (M = Co, Ni, Mn and Fe) and $LiFePO_4$. [5] In addition, boron is naturally abundant and environmentally benign. Further, triangle $(BO_3)^{3-}$ polyoxanions also has lighter mass compared to other polyoxanion groups $(XO_m)^{n-}$ reported for LIB such as $(AsO_4)^{2-}$, $(VO_4)^{2-}$, $(SO_4)^{2-}$, $(WO_4)^{2-}$, $(PO_4)^{2-}$, and $(SiO_4)^{2-}$. In addition, $(BO_3)^{3-}$ polyoxanions could deliver high output potential along with improved structural stability from inductive effect of B-O bond. Although $LMBO_3$ exhibited higher operating voltage and enhanced structural stability by keeping the benefit of networking anion group, they were suffered from low electrical conductivity similar to those of the olivine framework. The electrochemical activity of $LMBO_3$ was initially reported by Legagneur *et al.* along with low electrochemical activity. [5] While considering $LiFeBO_3$ is safer than $LiMnBO_3$, high capacity and high redox potential (~4.6 V)

than that of $LiFeBO_3$ (~ 3.2 V) makes $LiMnBO_3$ as more attractive candidate for LIB. Generally, $LiMnBO_3$ (LMB) exists in two polymorphs, which is either hexagonal (h-LMB) or monoclinic (m-LMB) phases. [6] It was reported by several researchers that m-LMB exhibited better electrochemical reactivity than h-LMB. [6-8] Kim *et al* observed high capacity of ~ 100 mAh g⁻¹ for m-LMB at low current density of C/20 in the second cycle. [6] Of late, several efforts had been taken to improve the electrochemical performance of LMB using carbon coating or making them composite with graphene. [7-11] Although the electrochemical activity of LMB was increased at low current densities, the high current rate performance is still not satisfactory to adopt them in large scale applications. It is well known that synthesis method played an important role to enhance the morphological feature thereby improving Li-ion storage behavior. [7, 10, 11] Apparently, utilization of nano-LMB, which reduced the pathway for Li-ion diffusion through its size effect and hence enhanced rate capability could be achieved. Moreover, forming highly conductive network between the nano-LMB is also an effective way to improve its inherent conductive properties and electrochemical reaction kinetics as well. [12] In this work, we have prepared monoclinic LMB nanobeads with ultra-thin carbon conductive network (LMB-NB) using urea assisted microwave irradiation method. Nevertheless, development of LMB-NB via microwave method has not been reported yet. The prepared materials had showed remarkable cycling performance even at high current rates, which is the best performance reported so far for LMB.

Monoclinic LMB-NB were prepared using microwave irradiation method with urea as surfactant as well as carbon sources. Stoichiometric amounts of lithium nitrate, manganese nitrate and boric acid were dissolved in 100 ml of distilled water. Then, an appropriate amount of urea was added to the above solution and stirred for 90 min. The molar ratio of metal ions to urea was fixed at 1:10. The resulting solution was heated in a domestic microwave oven (700 W, Daewoo, Korea) for 20 min, and then cooled to room temperature. Finally, the resultant product was fired at 650 °C for 7 h in an argon atmosphere to obtained LMB-NB powders. The phase analysis of LMB-NB was examined through X-ray diffraction measurements (XRD, Rint 1000, Rigaku, Japan) equipped with Cu-Kα as the radiation source. The morphological behavior of the LMB-NB was examined using a field emission transmission electron

microscope (TEM, Tecnai-F20, Philips, Netherland). Brunauer–Emmett–Teller (BET) surface area analysis was performed using an ASAP 2010 surface analyzer (Micromeritics, USA). The amount of carbon content in LMB-NB was determined by thermogravimetric analysis (TGA) from ambient temperature to 500 ^{o}C using a thermal analyzer system (STA 1640, Stanton Redcroft Inc., UK). The electrochemical performance individual LMB-NB was tested against a lithium counter electrode. The electrodes for half-cell were prepared by pressing a slurry of 80 % active material, 10 % ketzen black (KB) as conductive additive, and a 10 % Teflonized acetylene black (TAB with 7 wt % of Teflon) binder on a 200 mm^2 nickel mesh and dried at 160 °C for 4 h in an oven. The half-cells were fabricated in an argon filled glove box by sandwiching together a LMB-MB cathode and lithium anode separated by a separator (Celgard 3401) in 1 M LiPF$_6$ in a mixture of ethylene carbonate (EC) and dimethyl carbonate (DMC) (1:1 v/v, Soulbrain Co., Ltd, Korea) electrolyte. Electrochemical impedance spectroscopy (EIS) measurements were carried out using an electrochemical analyzer (SP-150, Bio-Logic, France). The charge/discharge test (C-DC) was performed in CR2032 type cell. The cathodes for the coin cell were prepared by pressing the mixture of 77 % LMB-NB, 11.5 % of Ketjen black and 11.5 % of Teflonized acetylene black (TAB) mixture on 150 mm^2 nickel mesh and dried at 160 ^{o}C for 4 h in a vacuum oven. The test cells were fabricated in an argon filled glove box by pressing a cathode and lithium metal anode separated by a porous polypropylene separator (Celgard 3401). 1 M LiPF$_6$ in 1:1 EC/DMC (v/v) was used as electrolyte. [12]

Fig 1a presented the XRD pattern of LMB-NB, which could be indexed based on monoclinic phase with C2/c space group according to the JCPDS card no. 83-2342.[5] Furthermore, narrow and highly indexed XRD peaks confirmed good crystalline nature of LMB-NB powders. The cell parameters a = 5.192 Å, b = 8.944 Å and c = 10.328 Å were observed and in good agreement with m-LMB. [10] In addition, the average crystallite size of powders grown by microwave irradiation method was found to be ~ 40 nm using Scherrer's formula. The presence of Mn^{2+} in LMB-NB was confirmed using electron paramagnetic resonance (EPR) as presented in Fig. 1b. The EPR of LMB-NB showed single broad line centered at 310.025 mT g ~ 2.00, indicating the existence of manganese ions in 2^{+} state. [13]
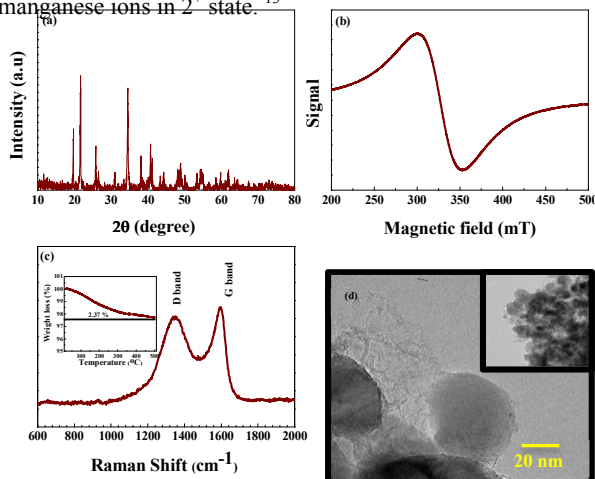
The Raman spectrum in fig 1c exhibited two broad peaks namely at ~ 1596 (G-band) and 1347 (D-band) cm^{-1}, which are characteristic for graphitic nature of carbon. The G-band originates from symmetric E$_{2g}$ vibrations mode of sp^2 atoms whereas the D-band is corresponds to the breathing mode of k-point phonons of A$_{1g}$ symmetry. The prominent peak at 1596 cm^{-1} can be attributed to disordered sp^3 bonded graphitic carbon, facilitating the improvement of ionic/electronic transfer of LMB-NB material. The BET surface area and carbon content in LMB-NB are calculated about 11 m^2 g^{-1} and 2.37 % (inserted in fig. 1c), respectively. It is clear from TEM image in fig. 2d that the LMB-NB power was composed of small and highly ordered particles (insert in fig. 2d) with average grain size of 30-40 nm. Moreover, each particle is interconnected well through ultra-thin porous carbon backbone, resulting from the combustion of urea, which also suppresses the particle growth during the synthesis process. This interconnected carbon network between LMB-NB is not only increases the conductive nature of LMB-NB, it also more allowed to store more electrolyte within LMB-NB structure, augmenting the structural stability against the inherent mechanical stress during the high current cycling process. It is well-known that the electrode material with high number of reaction sites, uniform particles with homogeneous size distribution and stable structure are essential parameters for improving the C-DC capability at high current rate.

The presence of carbon was confirmed using EDX and corresponding dot mapping was showed in fig. 2. The mapping of Mn in fig. 2b exhibited similar intensity distribution to B in fig 2c, demonstrating the homogeneity of LMB-NBs. Moreover, fig 2d showed the presence of homogeneously distributed carbon on the nanobeads. Besides, the selected area electron diffraction (SAED) pattern of LMB-NBs in fig 2e displayed bright spots, which could be indexed based on the interplanar spacings according to the monoclinic structure of LMB-NBs. [8]
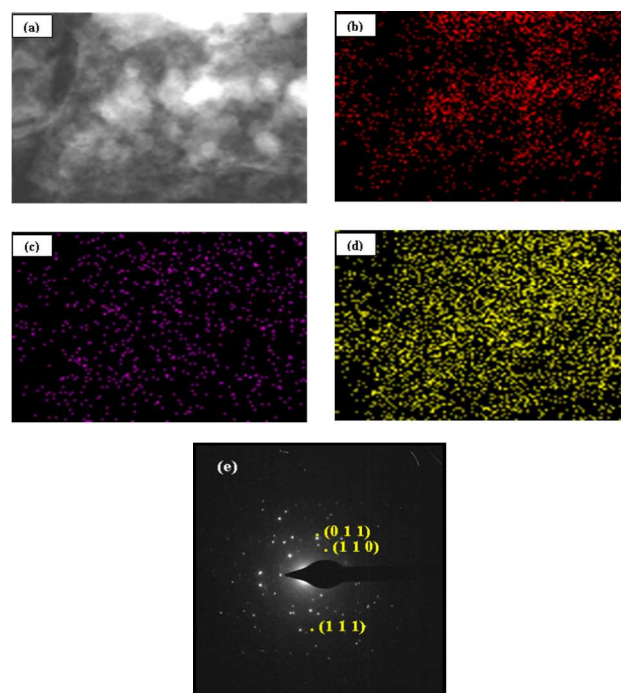

Fig. 1 (a) XRD pattern, (b) ESR, (c) Raman spectra and (d) TEM of LMB-NB prepared using urea assisted microwave irradiation method at 600 ^{o}C

Fig. 2 (a) TEM images of LMB-NB particles, (b) mapping of Mn, (c) mapping of B, (d) mapping of c coating layer and (e) SAED pattern of LMB-NB prepared using microwave irradiation method.

Fig. 3 represented the initial charge-discharge (C-DC) curves of the cells cycled between 1.25 - 4.8 V under ambient temperature at a C/20 rate. As seen from fig. 3 that the LMB-NB showed the sloped C-DC behaviour, in accordance with the other reports on the monoclinic LMB cathode.[11] The charge profile of LMB-NB revealed that about 0.75 mole of Li+ could be extracted from its structure at C/20 current rate up to 4.8 V, corresponding to the capacity of ~ 166 mAh g^{-1}. During discharge, ~ 0.54 mole of Li+ was reinserted into the LMB-NB structure, delivering a discharge capacity of ~ 120 mAh g^{-1}. It is clear that there was some irreversible capacity loss during the initial cycle, which may be attributed to the formation of solid-electrolyte interface film on the surface of the electrode material and electrolyte decomposition at high voltage.[5,14]
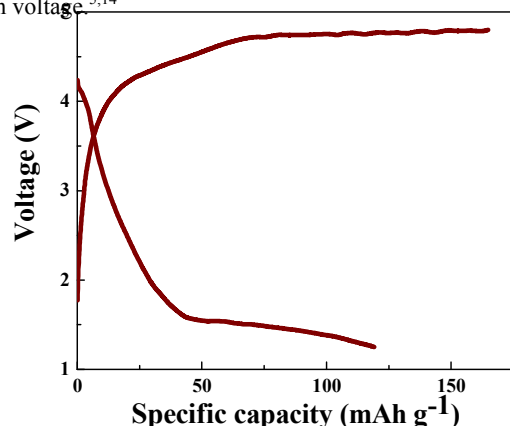

Fig. 3 Initial C-DC curve of LMB-NB electrode within 1.25-4.8 V at C/20 current rate

The discharge curves of Li$^+$/LMB-NB cell recorded within 1.25-4.8 V at different current densities are illustrated in fig 4a. The trend of C-DC curves are in well agreement with previous reports on LMB cathodes.[10, 11] Since (BO$_3$)$^{3-}$ polyanion has strong covalent bonding with metal ions, the high redox potential of Mn$^{3+/2+}$ couple could be resulted from the alternating the Mn$^{3+/2+}$ couple by polyanion.[5, 14] It well known that the lithium intercalation reaction kinetics at high current densities is low due to the reduced Li-ion diffusion process, since at high current rates the Li-ions approach only the outer surface of the electrode material. This is based on the diffusion effects of the Li-ion within the electrode material. Hence, it is held that part of the surface of the electrode materials contribute to a high charging/discharging rate, which decreased the voltage plateau at higher current rates, resulting low capacity value.[12] Although all the cells showed irreversible capacity loss during the initial cycle at all current densities, the columbic efficiency of the cell is over 96 % upon cycling process. A discharge capacities of 67, 64 and 55 mAh g^{-1} can be obtained at a current rate of 0.6, 1.5 and 4 C, respectively from Li$^+$/LMB-NB cell.

It is worth mentioning here that the capacity obtained in the present investigation is one of the best ever reported values for LMB cathode especially at high current rates.[5-7, 10, 11, 15] This superior electrochemical lithium storage performance is resulted from its morphological feature. The uniformly distributed LMB-NB along with ultra-thin porous carbon backbone could facilitate the Li-ion diffusion even at high current rates. On the other hand, nano sized LMB-NB also improved the contact between the particles/particles and the particles/current collector, ensuring the improvement of electrical conductivity and hence the lithium ion storage capability was enhanced.
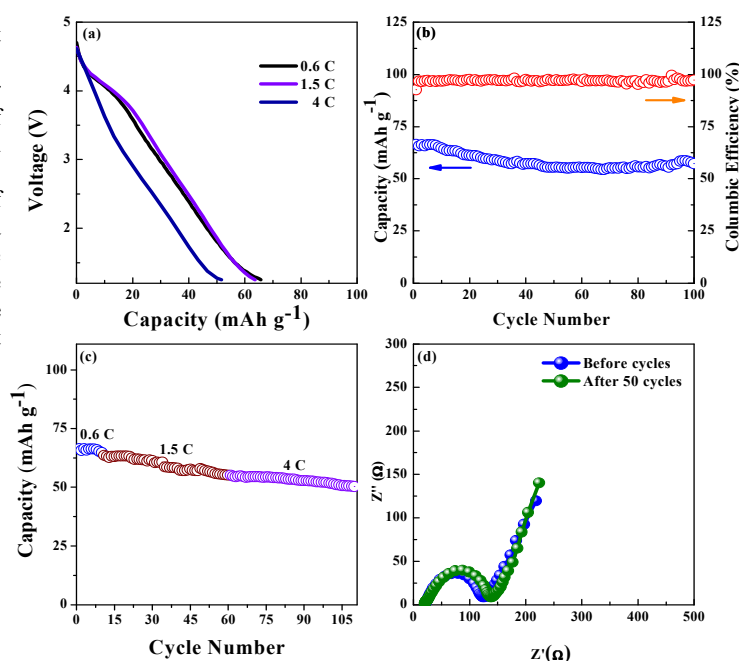

Fig. 4 (a) C/DC curves of Li$^+$/LMB-NB cell conducted between 1.25 and 4.8 V at different current rates, (b) cyclic performance of Li$^+$/LMB-NB cell at 0.6 C for 100 cycles, (c) rate capability of Li$^+$/LMB-NB cell at different current rates and (d) Nyquist spectra of Li$^+$/LMB-NB cell recorded before and after cycled at 4 C for 50 cycles.

The cycling performance at 0.6 C rate is presented in fig 4b. The cell exhibited ~ 88 % capacity retention at 0.6 C rate along with more than 96 % of coulombic efficiency. To the best of our knowledge, it is the best cycling performance for LMB powders prepared using various synthesis methods including solgel, spray drying, solid state and carbothermal reaction methods.[6-9, 11, 14] Furthermore, the Li$^+$/LMB-NB cell also displayed very stable cyclic performance at all current rates as presented in fig 4c. As observed from TEM analysis, the formation of ultra-thin porous carbon network between LMB-NB not only improves its conductivity, but also allowed to adsorb more electrolyte through the open carbon matrix and stabilizes the electrode/electrolyte interface, which improved the rate capability. In the meantime, electrolyte adsorption within LMB-NB structure also provided flexible structure against volume expansion/contraction during the cycling progress thus stabilized cycling performance even at high current rates.[12]

Nyquist spectra recorded before and after cycling at 4 C rate for 50 are given in Fig. 4d. As seen from Fig. 3d, the diameter of the semi-circle at low frequency region associated to the charge transfer resistance (R$_{ct}$) was slightly larger than that of before cycling, revealing that the increase in R$_{ct}$ value before and after cycled at high rate was relatively small. This outstanding cycling behavior at high current could result from the synergetic effect of improved intrinsic electronic and mechanical properties of the LMB-NB supported by ultra-thin porous carbon network, which correlated well with the results obtained from C/DC studies. Furthermore, negligible agglomeration and high crystalline nature of LMB-NB also aided the charge storage of Li$^+$/LMB-NB cell. These results clearly demonstrated that urea mediated microwave irradiation method could significantly enhanced both the conductivity and

electrochemical reaction kinetics of LMB-NB for high performance LIB applications.

Conclusions

The LMB-NB were synthesised using urea assisted microwave method and the possibility of utilizing them as high performance electrode materials for LIB was investigated against lithium counter electrode between 1.25 and 4.8 V at different current rates. The Li$^+$/LMB-NB cell delivered a discharge capacities of 67, 63 and 55 mAh g^{-1} at a current rate of 0.6 C, 1.5 C and 4 C, respectively along with excellent cyclic stability, which can be considered to be the best rate performance among other reports available on LiMNBO$_3$. The reason for the improved electrochemical performance could be concluded as follows: the formation of highly porous ultra-thin carbon network between LMB-NB particles supressed the particle agglomeration and increased the conductive nature of the materials as well as stabilized the solid-electrolyte interfacial layer, resulting in the excellent lithium storage behavior of LMB-NB electrode even at high current densities.

Notes and references

^{a} Department of Mechanical and Materials Engineering, The University of Western Ontario, London, Ontario, N6A 5B9, Canada.
^{b} Faculty of Applied Chemical Engineering, Chonnam National University, Gwang-ju 500-757, Korea.
E-mail: kkaliyap@uwo.ca, leeys@chonnam.ac.kr

1.   M. S. Whittingham, *Chemical Reviews*, 2004, **104**, 4271-4302.
2.   A. K. Padhi, K. S. Nanjundaswamy and J. B. Goodenough, *Journal of The Electrochemical Society*, 1997, **144**, 1188-1194.
3.   V. Aravindan, J. Gnanaraj, Y.-S. Lee and S. Madhavi, *Journal of Materials Chemistry A*, 2013, **1**, 3518-3539.
4.   P. G. Bruce, B. Scrosati and J.-M. Tarascon, *Angewandte Chemie International Edition*, 2008, **47**, 2930-2946.
5.   V. Legagneur, Y. An, A. Mosbah, R. Portal, A. Le Gal La Salle, A. Verbaere, D. Guyomard and Y. Piffard, *Solid State Ionics*, 2001, **139**, 37-46.
6.   J. C. Kim, C. J. Moore, B. Kang, G. Hautier, A. Jain and G. Ceder, *Journal of The Electrochemical Society*, 2011, **158**, A309-A315.
7.   Y.-S. Lee and H. Lee, *Electron. Mater. Lett.*, 2014, **10**, 253-258.
8.   S. Afyon, D. Kundu, F. Krumeich and R. Nesper, *Journal of Power Sources*, 2013, **224**, 145-151.
9.   R. Ma, L. Shao, K. Wu, M. Lao, M. Shui, C. Chen, D. Wang, N. Long, Y. Ren and J. Shu, *Ceramics International*, 2013, **39**, 9309-9317.
10.   K.-J. Lee, L.-S. Kang, S. Uhm, J. S. Yoon, D.-W. Kim and H. S. Hong, *Current Applied Physics*, 2013, **13**, 1440-1443.
11.   V. Aravindan, K. Karthikeyan, S. Amaresh and Y. S. Lee, *Bull. Korean Chem. Soc.* 2010, **31**, 1506-1509.
12.   K. Karthikeyan, S. Amaresh, V. Aravindan, W. S. Kim, K. W. Nam, X. Q. Yang and Y. S. Lee, *Journal of Power Sources*, 2013, **232**, 240-245.
13.   L. Pawlak, K. Falkowski and S. Pokrzywnicki, *Journal of Solid State Chemistry*, 1981, **37**, 228-231.
14.   L. Chen, Y. Zhao, X. An, J. Liu, Y. Dong, Y. Chen and Q. Kuang, *Journal of Alloys and Compounds*, 2010, **494**, 415-419.
15.   S. Li, L. Xu, G. Li, M. Wang and Y. Zhai, *Journal of Power Sources*, 2013, **236**, 54-60.